Numerical Supported Design of Continuously Adapted Riblets for Viscous Drag Reduction on a NREL Wind Turbine Airfoil

Karsten Oehlert
Jan H. Haake
Konrad M. Hartung
Institute of Energy and Process Engineering
Jade University of Applied Sciences
26389 Wilhelmshaven, Germany

KEYWORDS

Riblets, Drag reduction, Transition modeling, Wind turbines, Laser structuring.

ABSTRACT

Viscous drag is a significant factor contributing to the efficiency of aerodynamic application. During the last decades several studies have shown that functional surface structures provide the potential to reduce the viscous drag in the turbulent boundary layer and thus increase efficiency. Due to the rather challenging manufacturing process of micro-scale riblets most studies were conducted using constant riblet dimensions causing losses of the possible drag reduction. With the rapid development in micro structuring technologies it is now possible to manufacture continuously adapted riblets in almost industrial processing scales. For the design of continuously adapted riblets an algorithm is developed considering the effect of a deviation of the riblet spacing from its theoretical optimal value in order to maximize the cumulative drag reduction additionally effected by a misalignment of the riblet structure. The algorithm is applied for the design of riblets with a trapezoid cross-section for the NREL wind turbine airfoil S809 at a Reynolds number of $Re = 2 \cdot 10^6$. The shear stress data required to determine an appropriated region for the riblet application and optimal riblet dimensions are provided by 2D numerical studies using an empirical three equation transition model which shows good consistency of the predicted location of the transition onset with experimental results. With the outlined design approach an increased drag reduction in rage of 25.7% compared to riblets with constant dimensions can be expected.

INTRODUCTION

In most engineering and aerospace applications, such as airfoils, wind turbines or turbomachinery a transitional boundary layer flow occurs. The initially laminar boundary layer controlled by viscous forces becomes turbulent triggered by various types of sufficient flow disturbances. Within the turbulent boundary layer vortices naturally increase the momentum transfer and hence the viscous drag which is considered a major barrier to further optimization of aerodynamic performance. In the last three decades there has been extensive research on drag reduction techniques, mainly focusing on delaying the laminar-turbulent transition and modifying the turbulent structures in the boundary layer. As a passive drag reducing technique inspired by designs found throughout living nature, the dermal denticles of the skin of fast swimming sharks were found to produce low drag. In order to study the drag reducing effect in experimental fluid flow, most important characteristics have been identified and transcribed to simplified riblet geometries, including various types of blade, sawtooth, scalloped, and trapezoid cross-sections arranged periodically in wall flow direction. The extensive investigation on these micro-scale structures since the late 1970's e.g. by (Walsh 1980; Choi 1989; Walsh and Lindemann 1984; Bechert et al. 1997) have shown that riblets provide a drag reduction up to 10%. Furthermore, the experimental results of (Bechert et al. 1997) and (Bruse 1998) have shown that an adaption of the riblet dimensions to the local flow conditions is a basic requirement for an effective drag reduction by riblets. However due to the complex manufacturing process of micro-scale surface structures almost all experimental measurements were conducted using riblets with constant dimensions, such as provided by the 3M Corp. Therefore, the drag reducing potential of riblet structure could yet not be fully exploited. Thanks to the rapid development in micro structuring technology, especially in the field of high-rate laser micro processing (Loeschner et al. 2015; Schille et al. 2017) it is now possible to manufacture continuously adapted riblet in almost industrial processing scales. Aim of this paper is to present a numerical supported design process for continuously adapted riblets for the National Renewable Energy Laboratory (NREL) airfoil S809 for subsequent experimental and numerical investigations.

GENERAL INFORMATION ON RIBLETS

Drag Reducing Mechanism

In the near wall region, stripe-like turbulent structures arise whose middle axis of rotation are oriented in streamwise direction. These coherent vortices in

Proceedings 32nd European Conference on Modelling and Simulation ©ECMS Lars Nolle, Alexandra Burger, Christoph Tholen, Jens Werner, Jens Wellhausen (Editors)
ISBN: 978-0-9932440-6-3/ ISBN: 978-0-9932440-7-0 (CD)

the viscous sublayer were proven both by experimental (Kline et al. 1967; Clark 1990) and numerical results (Kim et al. 1987; Choi et al. 1993; Goldstein et al. 1995) . A flow visualization of the streamwise vortices was carried out by (Lee and Lee 2001) using a synchronized smoke-wire technique over a flat plate and a riblet structured surface with semicircular grooves (Figure 1). (Bechert et al. 1986) as well as (Bechert and Bartenwerfer 1989) assumed that the drag reducing effect of riblets is based on the blocking of the streamwise vortices in the near-wall region, which leads to a decreased momentum exchange in the vicinity of the wall. (Bhushan 2012) summarized the drag reducing effect of riblets as a coupled mechanism of blocking streamwise vortices in the viscous sublayer and an additional elevating effect towards the dominate vortices. The theory was later confirmed by direct numerical simulation of the boundary layer flow over riblet-structured surfaces e.g. by (Choi et al. 1993; Goldstein et al. 1995) as well as by experimental results (Vukoslavevi et al. 1992; Suzuki and Kasagi 1994) . Essential for an effective drag reduction is the correct dimensioning especially of the riblet spacing. In case of streamwise vortices in the near wall region with a middle diameter greater than the local riblet spacing, vortices are impeded and elevated resulting in a decreased momentum exchange in the near wall region. As the vortices only interact with the riblet tips, the overall wetted surface area in contact with fluid of high momentum is decreased leading to a significant viscous drag reduction (Vukoslavevi et al. 1992). For an oversized riblet spacing the streamwise vortices occur within the riblet valley. The overall wetted surface area in contact with fluid of high momentum is thereby increased resulting in a higher drag (Choi et al. 1993).

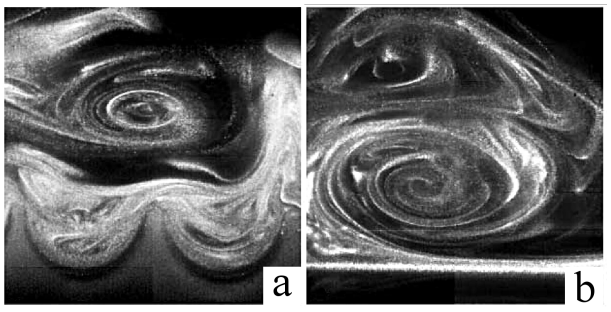

Fig. 1. Flow visualization of streamwise vortices in the turbulent boundary layer (Lee and Lee 2001): a) lateral cross-section of a smooth wall and b) lateral cross-section of riblets with semi-circular grooves

Impact of the Riblet Geometry

The geometrical characterization of riblets can be determined by the riblet spacing s, the riblet height h, the tip width t and the opening angle α. Furthermore, a misalignment angle φ is defined describing the misalignment between the riblet orientation and the freestream direction. For a better comparison of experimental data with various riblet geometries and flow conditions, non dimensional parameters measured in wall units, are introduced. These parameters are denoted by an additional $^+$-symbol as shown in Equation (1). Here, the expression τ_0 relates to the wall shear stress of a smooth reference surface.

$$s^+ = \frac{s}{\nu}\sqrt{\frac{\tau_0}{\rho}}; h^+ = \frac{h}{\nu}\sqrt{\frac{\tau_0}{\rho}}; t^+ = \frac{t}{\nu}\sqrt{\frac{\tau_0}{\rho}} \qquad (1)$$

The investigations of (Walsh 1982) and (Bechert et al. 1997) have shown that certain configurations of the riblet shape, the tip width, the riblet spacing and height maximize the achievable drag reduction. (Walsh 1982) showed in wind tunnel experiments that for riblets with a sawtooth cross-section the maximum drag reduction can be reached for a riblet height-to-spacing-ratio of h/s = 1. Later on (Bechert et al. 1997) discovered that the optimal height-to-spacing-ratio measured by (Walsh 1982) does not possess general validity. The systematic investigations of (Bechert et al. 1997) for various height-to-spacing-ratios showed that blade shaped and trapezoid shaped riblets exhibit a maximum drag reduction for a height-to-spacing-ratio of h/s = 0.5. Contrary riblets with semicircular grooves show a maximum drag reduction for a height-to-spacing-ratio of h/s = 0.7. Further investigations on the impact of the riblet shape and the riblet spacing on the drag reduction were carried out by (Bruse 1998). The results of the studies were later summarized by (Hage 2005) (Fig. 2). For riblets with a sawtooth cross-section, an opening angle of $\alpha = 60°$ and a height-to-spacing-ratio of approximately h/s $\approx$ 0.9 a maximum viscous drag reduction in range of $\triangle\tau/\tau_0 = -5,5\%$ was reached for a non dimensional riblet spacing of s^+ = 16. The overall highest reduction of viscous drag was measured for blade-shaped riblets with a height-to-spacing-ratio of h/s = 0.5 and a tip width of t = 0.02s. With this kind of cross section, a maximum drag reduction of $\triangle\tau/\tau_0 = -9,9\%$ was achieved for a non dimensional riblet spacing of s^+ =17. For riblets with a trapezoid cross-section a maximum drag reduction of $\triangle\tau/\tau_0 = -8,2\%$ was achieved with a height-to-spacing-ratio of h/s = 0.5 and a non dimensionlal riblet spacing of s^+ = 17. Due to the higher mechanical durability of riblets with trapezoid cross-section these should be preferred for practical applications. Furthermore the drag reducing effect of riblets shows a significant sensitivity towards the orientation relative to the flow direction as exemplary illustrated in Figure 3 for riblets with a trapezoid cross-section. The drag reduction reaches a maximum when the riblets are aligned in streamwise direction. In case of misalignment, the drag reduction decreases. Exceeding a certain misalignment angle leads to an increased surface friction compared to a smooth wall.

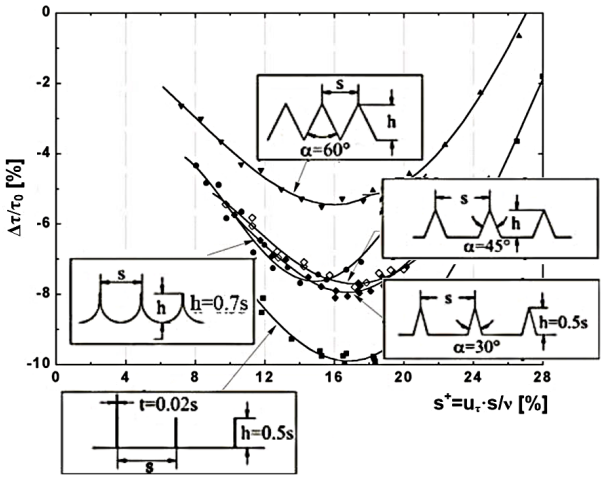

Fig. 2. Impact of the non dimensional riblet spacing on the relative change of the wall shear stress for various riblet shapes (Hage 2005)

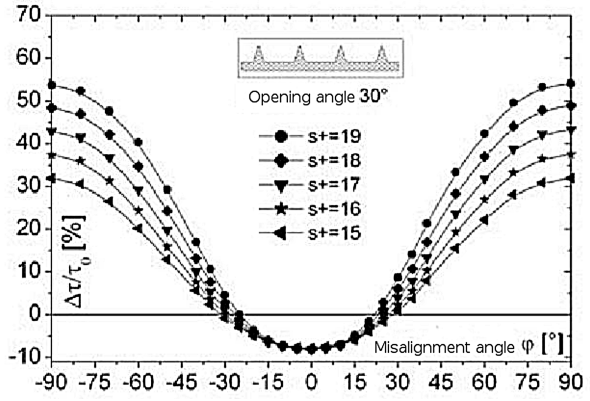

Fig. 3. Impact of the misalignment angle on the relative change of the wall shear stress for riblets with trapezoid cross-section (Hage 2005)

NUMERICAL SUPPORTED DESIGN OF CONTINOUSLY ADPADED RIBLETS

Riblets only lead to a drag reduction within the turbulent boundary layer while there height is within the viscous sublayer. The application of riblets within a laminar boundary layer would have a comparable impact as the application of a surface roughness increasing the overall viscous drag (Indinger 1999). Therefore, a subdivision of laminar, transitional and turbulent boundary layers is necessary to determine an appropriate area for the riblet application.

Transition Modeling

Presently turbulence and transitional phenomenona have still not been fully physically understood. In fact, most knowledge on turbulent flow is empirical. Therefore, a general model able to predict the transitional effects does not exist. To avoid the computational costs associated with solving the full transient Navier-Stokes equations, a number of empirical correlation based turbulence models, such as the $kk_L-\omega$ model and the $\gamma - Re_\Theta$ model have been developed showing promising results for the flat plate test cases as well as for flows over airfoils (Fürst, J. et al. 2013; Keith Walters and Cokljat 2008). The $kk_L-\omega$ turbulence model initially proposed by (Keith Walters and H. Leylek 2004) is based on $k-\omega$ framework which solves the two additional transport equations for the turbulent kinetic energy and the specific dissipation rate ω. Furthermore the $kk_L-\omega$ model solves a third transport equation for the laminar kinetic energy k_L to predict the magnitude of low frequency velocity fluctuations that have been identified triggering transition in the boundary layer (Keith Walters and Cokljat 2008). The model is based on the assumption that velocity fluctuations in the pre-transitional region can be divided into small-scale vortices contributing to turbulence production and large-scale longitudinal vortices contributing to the production of non-turbulent fluctuation. The transport equations for the turbulent kinetic energy, the laminar kinetic energy, and the specific dissipation rate are given by the Equations (2-4) and contain terms representing production, destruction, and transport mechanism. The production is expressed by the first term on the right hand side modeled by a small-scale eddy viscosity concept. The termsand appearing with opposite signs in the transport equations for laminar and turbulent kinetic energy are related to the transition mechanisms for bypass and natural transition, respectively. The terms and represent the non-isotropic part of the near wall dissipation of the turbulent and laminar kinetic energy. In the transport equation for the specific dissipation rate, the second term on the right hand side is the transition production term intended to reduce turbulent length scales during the transition process (Keith Walters and H. Leylek 2004). The fourth term on the right hand side decreases the length scale in the outer region of the turbulent boundary layer necessary to ensure an adequate prediction of the wake region (Keith Walters and H. Leylek 2003). In summary, the transition process is modelled by the effect of energy transfer from the laminar kinetic energy of large-scale longitudinal vortices to the turbulent kinetic energy of small-scale vortices with a concurrent reduction in turbulence length scale. A detailed overview of the model and the model constants is given by (Keith Walters and Cokljat 2008).

$$\frac{\mathrm{Dk_T}}{\mathrm{DT}} = P_{kT} + R_{BP} + R_{NAT} - D_T + \frac{\partial}{\partial x_j}\left[\left(v + \frac{\alpha_T}{\alpha_K}\right)\frac{\partial k_T}{\partial x_j}\right] - \omega k_T \qquad (2)$$

$$\frac{\mathrm{Dk_L}}{\mathrm{Dt}} = P_{kL} - R_{BP} - R_{NAT} - D_L + \frac{\partial}{\partial x_j}\left[v\frac{\partial k_L}{\partial x_j}\right] \qquad (3)$$

$$\frac{\mathrm{D}\omega}{\mathrm{Dt}} = C_{\omega 1}\frac{\omega}{K_T}P_{kT} + \left(\frac{C_{\omega R}}{f_w} - 1\right)\frac{\omega}{k_T}(R_{BP} + R_{NAT}) - C_{\omega 2}\omega^2 + C_{\omega 2}f_w\alpha_T f_w^2\frac{\sqrt{k_T}}{d^2} - \frac{\partial}{\partial x_j}\left[\left(v + \frac{\alpha_T}{\sigma_\omega}\right)\frac{\partial \omega}{\partial x_j}\right] \quad (4)$$

Numerical Setup

In this study the numerical supported design of continuously adapted riblets is conducted for the NREL wind turbine airfoil S809 designed for horizontal-axis wind turbines (HAWT). The coordinates of the airfoil were collected from NREL website and transferred into a 2D model by spline interpolation. The computational domain for the simulations consist of a semicircular section in the front with a radius of 10 chord lengths. The downstream distance of the computational domain from the airfoils leading edge is set to 21 chord lengths as illustrated in Figure 4. The semicircular as well as the bottom boundary were defined as velocity inlet. The top and downstream boundary were defined as pressure outlet. The number of cells and the near wall resolution of the C-type structured mesh were chosen such that the requirement of $y^+ < 1$ for the wall resolved turbulence modeling at a Reynolds number of $Re = 10^6$ and a velocity magnitude of 48m/s is satisfied. The inlet turbulence intensity and the turbulent viscosity ratio were set to 0.2% and 10, respectively. Simulations were conducted for an angle of attack ranging from 2° to 10° in intervals of 2° by adjusting the velocity components at the inlet. Steady state incompressible flow simulations were performed using the $kk_L - \omega$ turbulence model in the software environment Ansys.

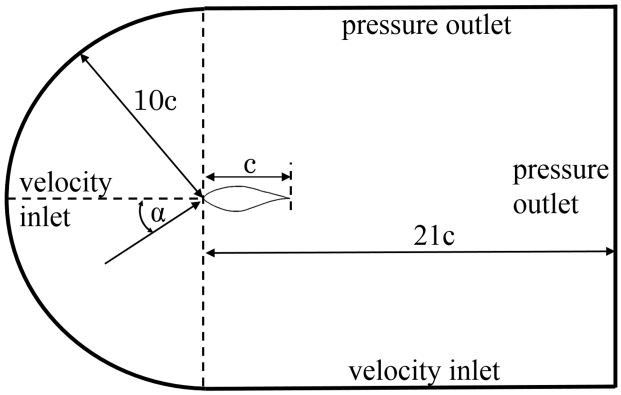

Fig. 4. Computational domain and boundary conditions for the 2D flow over an airfoil

2D Results

Based on the simulation setup discussed in the previous section, the numerical results were compared to the experimental data from (Somers 1997) in terms of the location of transition onset versus the angle of attack. According to the definitions of the $kk_L - \omega$ turbulence models the transition onset location was determined by an initially increasing turbulent kinetic energy in the near wall region. The numerical results show a good agreement of the predicted location and displacement for the transition onset with the experimental data (Figure 5 - 6). On the suction side, the location of transition onset steadily moves towards the leading edge of the airfoil with an accelerated displacement within the range between 5° and 9°. From an angle of approximately 8° on the location of transition onset remains apparently at the vicinity of the leading edge offering high potential for the drag reduction by riblets. On the pressure side the displacement for the location of transition onset shows an opposite behavior. With an increasing

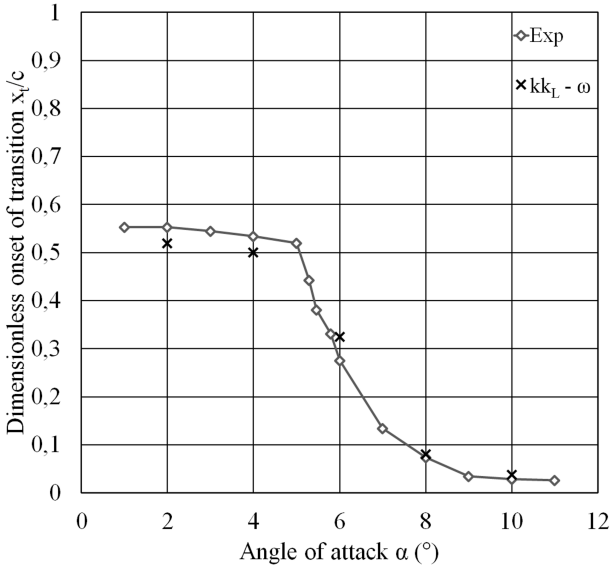

Fig. 5. Predicted and measured location of the transition onset on the suction side of the airfoil S809

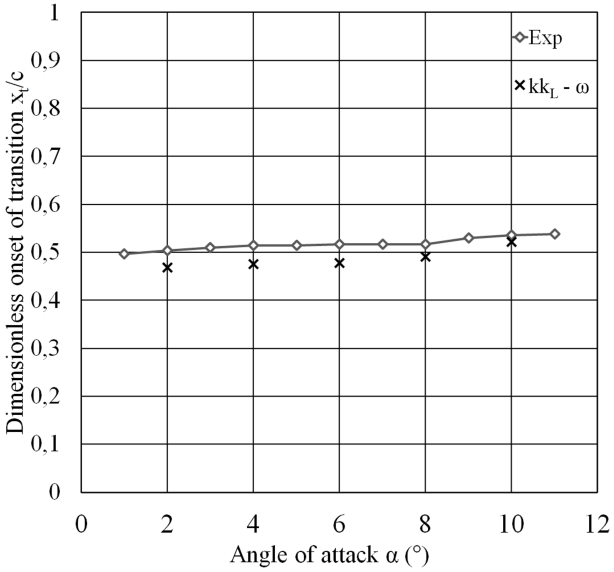

Fig. 6. Predicted and measured location of the transition onset on the pressure side of the airfoil S809

angle of attack the location of the transition onset moves towards the trailing edge of the airfoil showing an overall significant lower sensitivity compared to the suction side. Note that in literature, the location of transition onset is used for comparison of experimental and numerical result. For the selection of an appropriate area for the riblet application, however, information on the onset of the fully developed turbulent boundary layer is necessary. Therefore, the distribution of the wall shear stress as a function of the non dimensional airfoil length is computed and illustrated in Figure 7 together with the resulting classifications of laminar, transitional and turbulent boundary layers exemplary for an angle of attack of 8°.

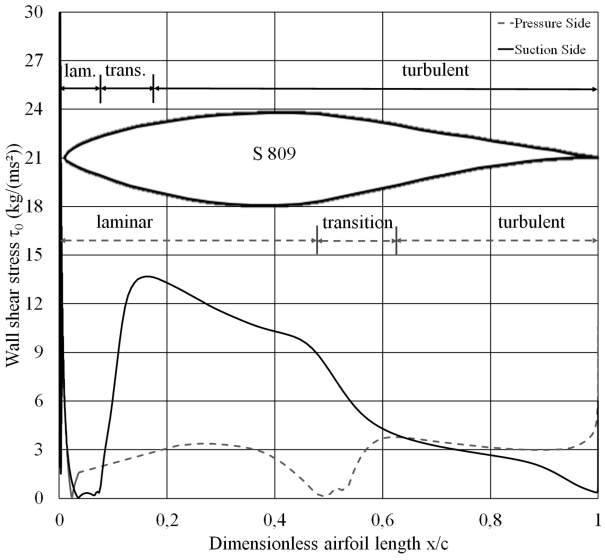

Fig. 7. Computed distribution of the wall shear stress on the smooth airfoil S809 at an angle of attack of 8°

Design of Continously Adapted Riblets

In accordance with the experimental results of (Lietmeyer et al. 2013), which show higher drag reducing potential of riblets on the suction side of an airfoil the design process of continuously adapted riblets is outlined for the suction side of the airfoil S809 at an angle of attack of 8°. Concerning the subsequent manufacturing process, the region between a non dimensional airfoil lengths of 0.2 and 0.95 seems appropriated of the riblet application. For the design process, a trapezoid riblet shape with an opening angle of $\alpha = 30°$, a non dimensional riblet spacing of $s^+ = 17$, and a riblet height that is determined by the local riblet spacing using $h = s/2$ is chosen. The theoretical optimal riblet spacing within the turbulent boundary layer can be determined by rewriting Equation (1) as

$$s = s^+ v \sqrt{\frac{\rho}{\tau_0}} \tag{5}$$

The resulting theoretical optimal riblet spacing based on the computed wall shear stress of the smooth airfoil is illustrated in Figure 8.

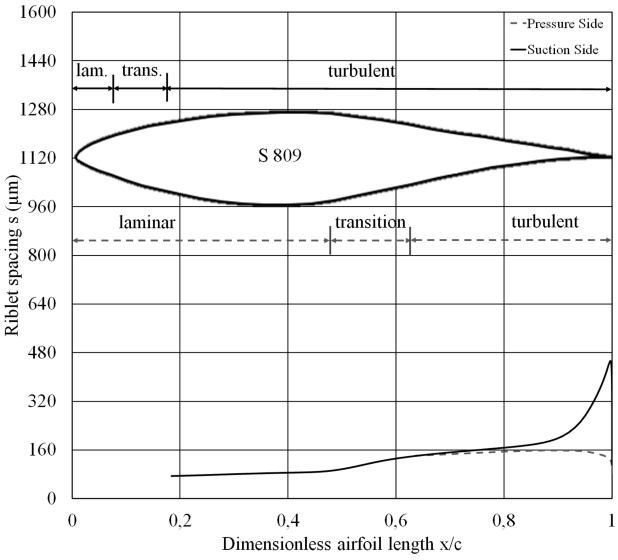

Fig. 8. Computed riblet spacing in the turbulent boundary layer for the smooth airfoil S809 at an angle of attack of 8°

The local varying riblet spacing leads inevitably to a local misalignment of the riblet orientation relative to the flow direction reducing the possible drag reduction as (Hage 2005) summarized (Figure 3). Therefore, a local deviation from the theoretical optimal non dimensional riblet spacing $s^+ = 17$ has to be considered in order to maximize the cumulative drag reduction. For this purpose, an algorithm was designed based on the experimental results of (Bechert et al. 1997) and (Bruse 1998) (cf. Fig. 2 - 3), which utilizes a polynomial approximation for the impact of the non dimensional riblet spacing and the misalignment angle on the drag reduction. To reduce the number of variables the misalignment angle is expressed in term of the local riblet spacing according to

$$\varphi = \arctan\left(\frac{s_{ij}(s^+) - s_{ij-1}}{x_{ij} - x_{i-1j}}\right), \tag{6}$$

whereby the index i is representing the streamwise and j the spanwise direction. By locally varying the non dimensional riblet spacing in Equation (5-6) and computing the corresponding drag reduction by the polynomial approximation the local misalignment angle and riblet spacing which minimize the cumulative drag can be identified. Nevertheless, the possible drag reduction of a riblet-structured surface with a continuously widening cross-section decreases in spanwise direction due to the increasing misalignment. Therefore, a abort criteria had to be considered, which terminates the structuring process in spanwise direction. The abort criteria was chosen in such a manner that an adding of further riblet structures in spanwise direction would lead to

a decreased drag reduction compared to the resulting drag when mirroring the structure in spanwise direction. To avoid additional stagnation points in the mirror plane an offset of the mirrored structures was provided. Figure 9 illustrates a segment of the continuously adapted riblet structure computed by the developed algorithm. For visual simplification a projection of the riblet structure on the curved surface of the airfoil was avoided. With this design approach a drag reduction of -8.02% would be possible. The application of riblets with constant dimensions computed based on the mean wall shear stress would result in a drag reduction of -6.38%. Therefore, through the application of continuously adapted riblets the drag reduction can be increased by 25.7% compared to constant riblet dimensions.

CONCLUSIONS

In this study a numerical supported design process for continuously adapted riblets is introduced. It is demonstrated that the correlation based transition $kk_L - \omega$ model can be successfully used to predict the location of the transition onset for the NREL S809 airfoil at various angle of attacks. However, it is not yet sufficiently investigated, if the $kk_L - \omega$ model provides accurate results for the wall shear stress distribution in the turbulent boundary layer, which is essential for the design process. Furthermore it is shown, that continuously adapted riblets require a deviation from the theoretical optimal riblet spacing in order to maximize the cumulative drag reduction. For the riblet structure generated by the developed algorithm an increased drag reduction of 25.7% in comparison to constant riblet dimensions can be expected. To prove evidence for the superior efficiency of the designed riblet structures the authors are currently exploring the drag reduction by numerical studies and experimental measurements.

ACKNOWLEDGEMENTS

This work has been conducted within the cooperative research project entitled *Fluidmechanical Optimization of Turbomachinery by High-rate Laser Structuring Technologies (OstrALas)* funded and supported by the German Federal Minister of Education and Research.

REFERENCES

Bechert, D. W. and Bartenwerfer, M. (1989). The viscous flow on surfaces with longitudinal ribs. *Journal of Fluid Mechanics*, 206:105129.

Bechert, D. W., Bartenwerfer, M., Hoppe, G., and Reif, W.-E. (1986). Drag reduction mechanisms derived from shark skin. 2:1044–1068.

Bechert, D. W., Bruse, M., Hage, W., van der Hoeven, J. G. T., and Hoppe, G. (1997). Experiments on drag-reducing surfaces and their optimization with an adjustable geometry. *Journal of Fluid Mechanics*, 338:5987.

Bhushan, B. (2012). *Biomimetics Bioinspired Hierarchical Structured Surfaces for Green Science and Technology*. Springer Verlag.

Bruse, M. (1998). *Zur Strömungsmechanik wandreibungsvermindernder riblet-Oberflächen*. Fortschritt-Berichte VDI. Reihe 7, Strömungstechnik. VDI-Verlag.

Choi, H., Moin, P., and Kim, J. (1993). Direct numerical simulation of turbulent flow over riblets. *Journal of Fluid Mechanics*, 255:503539.

Choi, K.-S. (1989). Near-wall structure of a turbulent boundary layer with riblets. *Journal of Fluid Mechanics*, 208:417458.

Clark, D. G. (1990). Boundary layer flow visualisation patterns on a riblet surface. In Coustols, E., editor, *Turbulence Control by Passive Means*, pages 79–96, Dordrecht. Springer Netherlands.

Fürst, J., Straka, P., Phoda, J., and imurda, D. (2013). Comparison of several models of the laminar/turbulent transition. *EPJ Web of Conferences*, 45:01032.

Goldstein, D., Handler, R., and Sirovich, L. (1995). Direct numerical simulation of turbulent flow over a modeled riblet covered surface. *Journal of Fluid Mechanics*, 302:333376.

Hage, W. (2005). Zur widerstandsverminderung von dreidimensionalen riblet-strukturen und anderen oberflchen. (dissertation).

Indinger, T. (1999). Einfluss von riblets auf die natrliche transition von grenzschichten. Technical report, Technical University of Dresden.

Keith Walters, D. and Cokljat, D. (2008). A three-equation eddy-viscosity model for reynolds-averaged navierstokes simulations of transitional flow. *Journal of Fluids Engineering*, 130:121401 121401 14.

Keith Walters, D. and H. Leylek, J. (2003). A cfd study of wake-induced transition on a compressor-like flat plate. 6.

Keith Walters, D. and H. Leylek, J. (2004). A new model for boundary layer transition using a single-point rans approach. *Journal of Turbomachinery*, 126:193 202.

Kim, J., Moin, P., and Moser, R. (1987). Turbulence statistics in fully developed channel flow at low reynolds number. *Journal of Fluid Mechanics*, 177:133166.

Kline, S. J., Reynolds, W. C., Schraub, F. A., and Runstadler, P. W. (1967). The structure of turbulent boundary layers. *Journal of Fluid Mechanics*, 30(4):741773.

Lee, S.-J. and Lee, S.-H. (2001). Flow field analysis of a turbulent boundary layer over a riblet surface. *Experiments in Fluids*, 30(2):153–166.

Lietmeyer, C., Oehlert, K., and Seume, J. R. (2013). Optimal application of riblets on compressor blades and their contamination behavior. *Journal of Turbomachinery*, 135:011036 011036 10.

Loeschner, U., Schille, J., Streek, A., Knebel, T.,

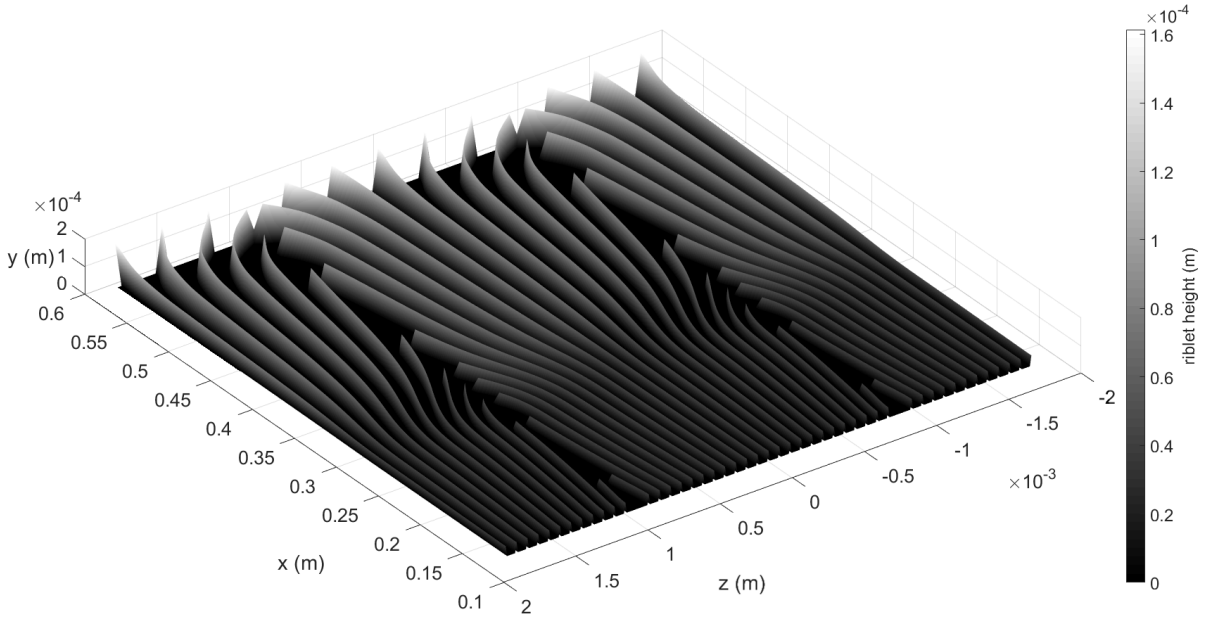

Fig. 9. Segment of the computed continuously adapted riblet structure for the suction side of the S809 airfoil

Hartwig, L., Hillmann, R., and Endisch, C. (2015). High-rate laser micro processing using a polygon scanner system. *Journal of Laser Application*, 27:29303 1 7.

Schille, J., Schneider, L., Hartwig, L., and Loeschner, U. (2017). High rate laser processing of metals using high-average power ultrashort pulse laser. *Journal of Laser Application*, 36:31 50.

Somers, D. (1997). Design and experimental results for the s809 airfoil. (WE711110).

Suzuki, Y. and Kasagi, N. (1994). Turbulent drag reduction mechanism above a riblet surface. 32:1781–1790.

Vukoslavevi, P., Wallace, J., and Balint, J.-L. (1992). Viscous drag reduction using streamwise-aligned riblets. 30:1119–1122.

Walsh, M. (1980). Drag characteristics of v-groove and transverse curvature riblets. 72.

Walsh, M. (1982). Turbulent boundary layer drag reduction using riblets. 6:82–169.

Walsh, M. and Lindemann, M. (1984). Optimization and application of riblets for turbulent drag reduction.

AUTHOR BIOGRAPHIES

KARSTEN OEHLERT graduated at the Leibniz University of Hannover, Germany, in 2005. He received his Dr.-Ing. degree in 2011 for the investigation of drag reducing riblet structures on compressor blades at the Institute of Turbomachinery and Fluid Dynamics. From 2009 to 2013 he worked for the E.ON AG in the *Department of System Technology and Security Analysis*. In the years 2013-2015 he was employed at the Volkswagen Group in the department of R&D in Wolfsburg. Presently he is Professor for Turbomachinery at the Institute of Energy and Process Engineering at the Jade University of Applied Science in Wilhelmshaven, Germany and in this function in the leadership of the cooperative research project *OstrALas* funded by the Federal Ministry of Education and Research. His research interests are mainly in the fields of turbomachinery, fluidmechanics and boundary layer subjects.
His email address is: karsten.oehlert@jade-hs.de.

JAN H. HAAKE received his bachelor in mechanical engineering in 2017. Presently he is studying for a master degree in mechanical engineering.
His email address is: Jan.Haake@student.jade-hs.de.

KONRAD M. HARTUNG received his Master of Science in mechanical engineering in 2016 from the Leibniz University of Hannover. Since 2017 he is working as scientific assistant in the area of computational fluid dynamics at the Jade University of Applied Science in Wilhelmshaven, Germany. He is part of the research project OstrALas funded by the Federal Ministry of Education and Research.
His email address is: konrad.hartung@jade-hs.de.